TOPOGRAPHY OF THE 81/PWILD 2 NUCLEUS DERIVED FROM STARDUST STEREOIMAGES. R. L. Kirk[1], T. C. Duxbury[2], F. Hörz[3], D. E. Brownlee[4], R. L. Newburn[2], P. Tsou[2], and the Stardust Team, [1] U. S. Geological Survey, Flagstaff, AZ 86001, U.S.A. (rkirk@usgs.gov), [2] Jet Propulsion Laboratory, California Institute of Technology, Pasadena, CA 91109. U.S.A., [3] NASA Johnson Space Center, Houston, TX, 77058, U.S.A., [4] Dept. of Astronomy, Univ. of Washington, Seattle, WA 98195, U.S.A.

Introduction: On 2 January, 2004, the Stardust spacecraft flew by the nucleus of comet 81P/Wild 2 with a closest approach distance of ~240 km. During the encounter, the Stardust Optical Navigation Camera (ONC) obtained 72 images of the nucleus with exposure times alternating between 10 ms (near-optimal for most of the nucleus surface) and 100 ms (used for navigation, and revealing additional details in the coma and dark portions of the surface [1,2]. Phase angles varied from 72° to near zero to 103° during the encounter, allowing the entire sunlit portion of the surface to be imaged. As many as 20 of the images near closest approach are of sufficiently high resolution to be used in mapping the nucleus surface; of these, two pairs of short-exposure images were used to create the nucleus shape model and derived products reported here. The best image resolution obtained was ~14 m/pixel, resulting in ~300 pixels across the nucleus. The Stardust Wild 2 dataset is therefore markedly superior from a stereomapping perspective to the Deep Space 1 MICAS images of comet Borrelly [3]. The key subset of the latter (3 images) covered only about a quarter of the surface at phase angles ~50°–60° and less than 50 x 160 pixels across the nucleus, yet it sufficed for groups at the USGS and DLR to produce digital elevation models (DEMs) and study the morphology and photometry of the nucleus in detail [4,5].

Comet Wild 2: Wild 2 is a Jupiter Family Comet that was captured into an inner solar system orbit only 30 years ago as the result of an encounter with Jupiter [6]. Thus, although the nucleus is likely evolving rapidly at present, it might have been less extensively modified to date than the other comet nuclei that have been imaged, 1P/Halley and 19P/Borrelly. Certainly, the appearance of the Wild 2 nucleus was strikingly different from these objects in several respects. Its gross shape resembles a triaxial ellipsoid quite closely, and the best fitting ellipsoid is somewhat prolate [1] (more precisely, "bar-of-soap" shaped, with three axes of distinct lengths). In contrast, Halley and Borrelly are prolate (middle axis similar to short axis) but less regular in shape. Over short distances (≤ 1 km), the surface of Wild 2 is rugged and is covered with a large number of circular or nearly circular depressions (craters, in the nongenetic sense) that are not resolved on the other comets. Several distinct crater morphologies have been described, with impact and nonimpact origins ascribed to different classes [1]. Other topographic features include ridges, pinnacles, blocks, and possible overhangs, many of which appear to be extremely steep. With few exceptions, brightness patterns on Wild 2 appear to be related to topographic shading; the albedo (and fine compositional/textural properties that affect brightness) appear to be much more uniform than on Borrelly [4,5].

Methodology: The starting point for our work is stereoanalysis of the ONC images because this technique, with its rigorous basis in geometry, provides the most accurate feature coordinates. Mapping was carried out with a synergistic combination of the USGS in-house digital cartography system ISIS [7], used for image ingestion and calibration, and our commercial digital photogrammetric workstation running BAE Systems' SOCET SET software [8] for control, automatic DEM production, and interactive DEM editing using the system's stereo display. Additional third party software such as ESRI ArcGIS is used to visualize and analyze the results and format them for presentations. This collection of software systems and the procedures used are similar to those we have applied to numerous other planetary datasets in the past several years, in particular in our modeling of the Borrelly nucleus with Deep Space 1 MICAS images of Borrelly [4]. Based on this experience and on the resolution of the ONC images, we expected to be able to produce DEMs with a horizontal resolution of ~50 m (3 image pixels) and a vertical precision on the order of 6 m.

The SOCET SET software is optimized for mapping regions much smaller than the planetary radius from a given image pair, whereas images of small solar-system bodies (including Wild 2) typically show the entire facing hemisphere of the nucleus. Rather than attempting to use body-centered geographic (latitude and longitude) coordinates, we therefore find it convenient to establish a Cartesian coordinate system and collect shape data in the form of an array of Z-coordinate values for points uniformly spaced in the X-Y plane. The X, Y, Z coordinates of individual points can then be transformed to other coordinate systems of interest, as described below. The primary coordinate system used for modeling Wild 2 has its +X axis in the direction of spacecraft motion relative to the nucleus, +Z axis in the direction from the nucleus to the point of closest approach, and +Y axis completing a righthanded set. In this coordinate system the Sun is approximately in the XZ plane, 16° in the –X (inbound) direction from the Z axis. Most of the illuminated area of the nucleus is on the "top" surface (largest Z value at given X and Y) and was mapped as a single raster based on image pairs N2069WE01/ N2071WE01 (spacecraft positions 48° and 31° from Z toward -X, respectively) and N2075WE01/ N2077WE01 (spacecraft 22° and 43° from Z toward +X). This surface is shown in Figure 1. A few small areas on the "bottom" surface in Cartesian coordinates were mapped separately, based on the pre-approach pair 2069/2071.

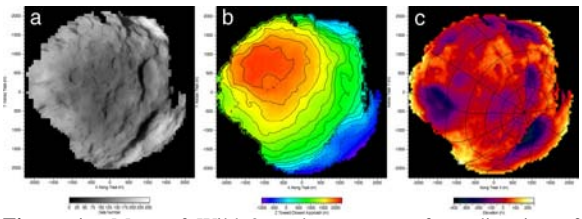

Figure 1. Maps of Wild 2 nucleus as seen from direction of closest approach. (a) Orthorectified image, highpass filtered to reduce limb-to-terminator brightness gradients. Equant shape of nucleus viewed from this direction gives little indication of its true dimensions. (b) Color-coded contour map of Z coordinate (toward closest approach) from –1000 to 2500 m with 200 m interval emphasizes overall rounded shape with minor local variations that are difficult to relate to the image. (c) Color-coded elevations from –400 to 250 m normal to best-fit ellipsoid clearly show major surface depressions as well as highstanding areas between. Graticule with 15° latitude, 30° longitude interval is also shown.

Shape and Size: The axes, orientation, and position of a triaxial ellipsoid were adjusted to yield a least-squares fit to the Cartesian coordinates of a total of 5576 surface points determined by stereoanalysis. Because the data cover nearly half the nucleus and conform quite closely to the ellipsoid, all 9 parameters could be determined robustly. This situation contrasts strongly with the modeling of Borelly, for which the Z coordinate of the body center was a matter of almost pure conjecture, based only on the depth of the visible surface.

The semiaxes of the fitted ellipsoid are 2.607, 2.002, and 1.350 km, which may be compared to the values 2.75, 2.00, and 1.65 ±0.05 km reported in [1]. We have not estimated the formal uncertainty in our axes, but it is likely to be comparable to the amplitude of topography relative to the ellipsoidal shape, which is described below. We would also expect our model to be systematically smaller than that of [1] because it is a fit to the data whereas the earlier model was constructed as an envelope enclosing the highest points on the surface. Allowing for both random error and systematic size difference at the ~100 m level, we find the major and middle axes to agree closely with the previously given values, but the minor axis to be distinctly shorter. This axis is the most difficult to determine because the nucleus was illuminated and viewed almost entirely from one of its ends. The volume of our ellipsoid is about 80% of that given in [1].

The J2000.0 celestial coordinates of the short (body Z) axis, which can be considered the negative rotational pole, are RA 292°, Dec 17°. This orientation differs by 5° from that given in [1] and 3° from that of [2].

Topography and Slopes: The stereoscopically determined coordinates of the surface points were translated and rotated to a body-centered system with X, Y, and Z axes along the long, middle, and short axes of the fitted ellipsoid, respectively.

Planetocentric latitudes and longitudes as well as elevations measured normal to the reference ellipsoid could then be computed. Figure 1c shows the elevation data viewed from the direction of closest approach, and Figure 2 shows four views along the -X, ±Y, and +Z axes of the ellipsoid (the remaining two views are omitted because they contain few points). Elevations range from -400 m in the depression referred to (unofficially; see [1]) as Shoemaker basin to +250 m nearby, with a mean of 0, mode of ~50 m, and RMS variation of 86 m. The distribution of elevations is smooth and unimodal (though slightly skewed); although there is some suggestion of layering in the images, this does not translate into a resolvable preference for some absolute elevations over others, indicating that the layering is not globally consistent.

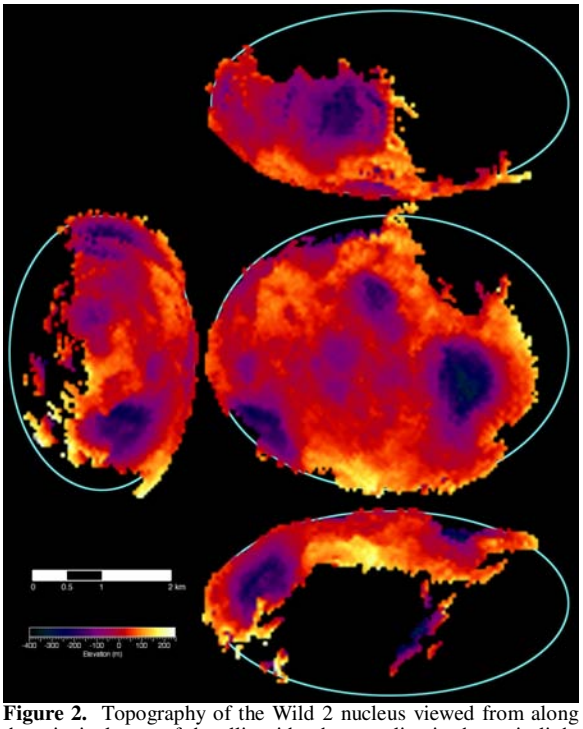

Figure 2. Topography of the Wild 2 nucleus viewed from along the principal axes of the ellipsoid, whose outline is shown in light blue.

A quantitative assessment of the properly area-weighted probability distribution of surface slopes on the nucleus is challenging because the known points are spaced very irregularly on the ellipsoid, which is, itself, highly nonspherical. As a first look at slopes, we have isolated profiles across the nucleus and computed elevations and arc lengths with respect to a best-fit ellipse that can then be used to compute bidirectional slopes. Slopes up to 75° are seen in a few places (though these are probably affected significantly by the finite resolution of the images and hence the shape model), with a RMS value near 25°. These results quantitatively confirm the conclusions of [1] about the extreme slopes and overall ruggedness of the nucleus. These slopes are extremely rugged compared to most other solar-system bodies, and strongly suggest that there is little unconsolidated material on Wild 2 and that the dominant erosive process involves sublimation rather than mass wasting. Some individual depressions appear distinctly asymmetric in the elevation and slope profiles, an artifact caused by the absence of any datapoints inside the shadowed portion of the depressions.

Craters: The most prominent features in the Wild 2 stereo topographic model are quasi-circular craters, which range in diameter from a few hundred meters to several kilometers. We measured the depths *d* and diameters *D* of 23 depressions >200 m that could be identified based on the on-axis views of the topography (Fig. 2) without reference to the images. Diameters were measured as the three-dimensional straight-line distance between two selected points on the opposite rims of the crater; this process is somewhat subjective in that visibility of the crater edges is affected by the false-color scheme used. It also results in significantly larger diameters for the largest basins (e.g., 2.4 vs. 1.6 km for Shoemaker) than the two-dimensional estimates in [1]. Depths were computed as the difference between the ellipsoid-relative height at the deepest point in the crater interior and that of a representative point on the rim. Results are shown in Figure 3. The d/D ratio, which is essentially independent of size, is comparable to that of fresh, bowl-shaped lunar craters [9] (as well as small fresh craters on the terrestrial planets), and substantially greater than for craters on other small bodies [10]. It is important to note that Fig. 3 includes measurements of both flat-floored and more complex "pit-halo" craters [1], which are morphologically distinct from one another and from bowl-shaped impact craters. The figure also includes measurements for the features "Left Foot" and "Right Foot", which were described in [1] as complex and potentially highly modified by nonimpact processes. In the Z-axis view (Fig. 2, center), these features each appear to consist of two partially overlapping, nearly circular, flat-floored depressions. We therefore feel justified in treating the "sole" and "heel" of each foot as a separate crater. In any case, the d/D ratios obtained do not, by themselves, distinguish different classes of craters. The depth of craters on Wild 2 will hopefully serve as a useful constraint on future theories of their formation and modification.

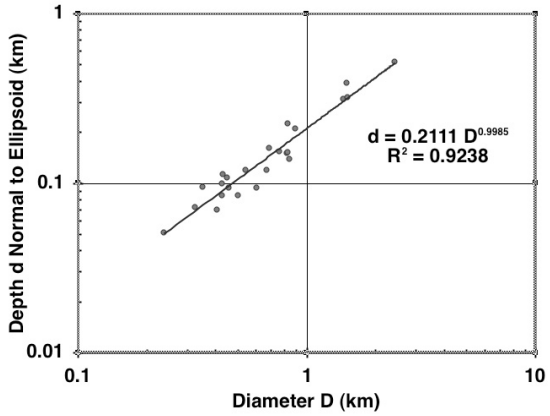

Figure 3. Diameters and depths (normal to ellipsoid) of 23 craters on the Wild 2 nucleus. Power-law fit indicates essentially constant depth/diameter ratio of 0.2, similar to simple lunar craters [9].

Next Steps: We are analyzing pairs of long-exposure images in an attempt to measure surface coordinates in the shadowed areas of the nucleus. By collecting data in coordinates rotated about the cross-track axis, we will also be able to increase the density of datapoints in regions that are not well seen from the point of closest approach, further improving our slope estimates.

Completion of the radiometric calibration of the images will make possible a series of photometric investigations similar to those for Borrelly [4]. Modeling of photometric effects, including both limb darkening and brightness as a function of phase angle, will yield information about surface particles and textures. Comparison of the images with models computed from the topography will allow us to assess local variations in albedo and roughness. Finally, we will be able to use photoclinometry [11] as a form of "smart interpolation" to make topographic models that resolve single-pixel details. With such models it will be possible to measure the morphometry of additional, smaller craters and to begin quantitative studies of the enigmatic small features of Wild 2 such as layering, pinnacles, and apparent overhangs.

References: [1] Brownlee D. E. et al. (2004) *Science, 304*, 1764. [2] Sekanina Z. et al. (2004) *Science, 304*, 1769. [3] Soderblom L. A. et al. (2003) *Icarus, 167,* 4. [4] Kirk R. L. et al. (2004) *Icarus, 167*, 54. [5] Oberst J. et al. (2004) *Icarus, 167*, 259. [6] Sekanina Z. and Yeomans K. (1985) *Astron. J., 85*, 2334. [7] Eliason E. (1997) *LPS XXVIII*, 331; Gaddis L. R. et al. (1997) *LPS XXVIII*, 387; Torson J. and Becker K. (1997) *LPS XXVIII*, 1443. [8] Miller S. B. and Walker A. S. (1993) *ACSM/ASPRS Ann. Conv. Expos. Tech. Papers, 3*, 256; Miller S. B. and Walker A. S. (1995) *Z. Photogr. Fernerkundung, 1*(95), 4. [9] Pike R. J. (1977) in *Impact and Explosion Cratering*, Pergamon, 489. [10] Carr M. H. et al. (1994) *Icarus, 107*, 61; Sullivan R. et al. (1996) *Icarus, 120*, 119; Thomas P. C. et al. (2002) *Icarus, 155*, 18. [11] Kirk R. L. et al. (2003) online at http://astrogeology.usgs.gov/Projects/ISPRS/Meetings/Houston2003/abstracts/Kirk_isprs_mar03.pdf.